



1	2
3	4
5	6
7	8
9	10
11	12
13	14
15	16
17	18
19	20
21	22
23	24
25	26
27	28
29	30
31	32
33	34
35	36
37	38

Variational Methods in Biomedical Imaging

Part III: Applications

Luis Pizarro

Biomedical Image Analysis Group
Department of Computing
Imperial College, London, UK

Outline

Outline

- ◆ Restoration
- ◆ Deblurring
- ◆ Optic Flow
- ◆ Reconstruction

1	2
3	4
5	6
7	8
9	10
11	12
13	14
15	16
17	18
19	20
21	22
23	24
25	26
27	28
29	30
31	32
33	34
35	36
37	38



Combined 1st- and 2nd-order regularisation

Didas 2004

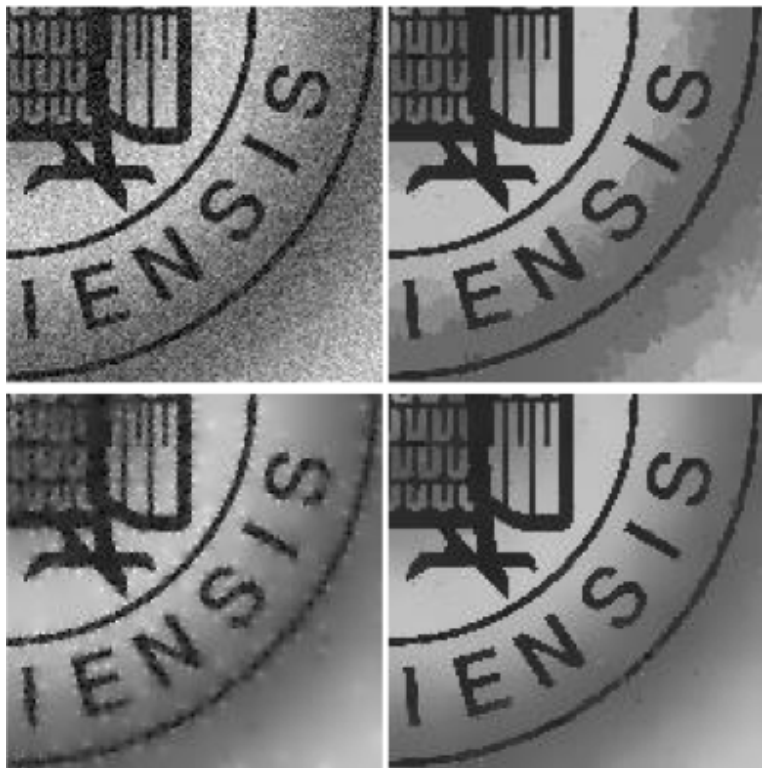
$$\min_u \int_{\Omega} \left((u - f)^2 + \alpha \Psi_1(|\nabla u|^2) + \beta \Psi_2((\Delta u)^2) \right) dx$$

Solved via the PDE

$$\frac{\partial u}{\partial t} = (\mathbf{f} - \mathbf{u}) + \alpha \operatorname{div}(\Psi'_1(|\nabla u|^2) \nabla u) - \beta \Delta(\Psi'_2((\Delta u)^2) \Delta u)$$

Using the non-convex Perona-Malik penaliser

$$\Psi_1(s^2) = \Psi_2(s^2) = 2\lambda^2 \log\left(1 + s^2/\lambda^2\right)$$



Variational restoration with higher-order regularisation. **Top left:** Noisy input image, **Top right:** 1st-order, **Bottom left:** 2nd-order, **Bottom right:** combined 1st- and 2nd-order. Source: Didas 2004.

1	2
3	4
5	6
7	8
9	10
11	12
13	14
15	16
17	18
19	20
21	22
23	24
25	26
27	28
29	30
31	32
33	34
35	36
37	38



1	2
3	4
5	6
7	8
9	10
11	12
13	14
15	16
17	18
19	20
21	22
23	24
25	26
27	28
29	30
31	32
33	34
35	36
37	38



The ROF Model

Rudin et al. 1992

$$\min_u \int_{\Omega} \left(|\nabla u|_1 + \frac{\lambda}{2}(u - f)^2 \right) dx$$

- ◆ Discrete **primal**

$$\min_u \left\{ F(Du) + G(u) \right\}$$

reads

$$\min_u \left(\|\nabla u\|_1 + \frac{\lambda}{2}\|u - f\|_2^2 \right)$$

- ◆ Discrete **primal-dual**

$$\min_u \max_p \left\{ \langle Du, p \rangle + G(u) - F^*(p) \right\}$$

reads

$$\min_{u \in X} \max_{p \in Y} \left(- \langle u, \operatorname{div} p \rangle_X + \frac{\lambda}{2}\|u - f\|_2^2 - \delta_P(p) \right)$$



- ◆ Discrete **primal-dual**

$$\min_{u \in X} \max_{p \in Y} \left(- \langle u, \operatorname{div} p \rangle_X + \frac{\lambda}{2}\|u - f\|_2^2 - \delta_P(p) \right)$$

then

$$F : \min_p \left(\frac{\|p - q\|^2}{2} + |p| \right) \longrightarrow \text{Pointwise shrinkage}$$

$$p = (I + \sigma \partial F^*)^{-1}(\tilde{p}) \iff p_{i,j} = \frac{\tilde{p}_{i,j}}{\max(1, |\tilde{p}_{i,j}|)}$$

$$G : \min_x \left(\frac{\|x - z\|^2}{2} + \lambda/2(x - f)^2 \right) \longrightarrow \text{Pointwise quadratic problem}$$

$$u = (I + \tau \partial G)^{-1}(\tilde{u}) \iff u_{i,j} = \frac{\tilde{u}_{i,j} + \tau \lambda f_{i,j}}{1 + \tau \lambda}$$

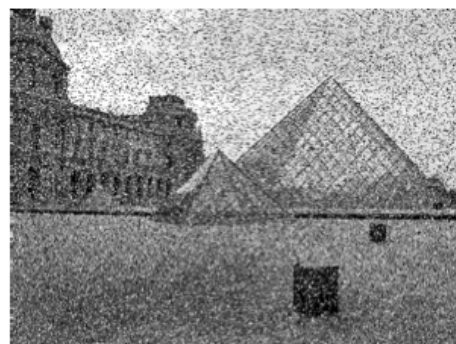
1	2
3	4
5	6
7	8
9	10
11	12
13	14
15	16
17	18
19	20
21	22
23	24
25	26
27	28
29	30
31	32
33	34
35	36
37	38

1	2
3	4
5	6
7	8
9	10
11	12
13	14
15	16
17	18
19	20
21	22
23	24
25	26
27	28
29	30
31	32
33	34
35	36
37	38

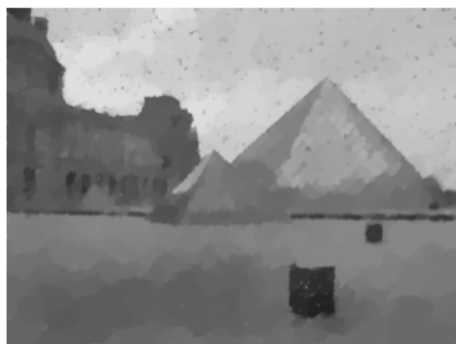
Image Restoration



(a) Clean image



(b) Noisy image



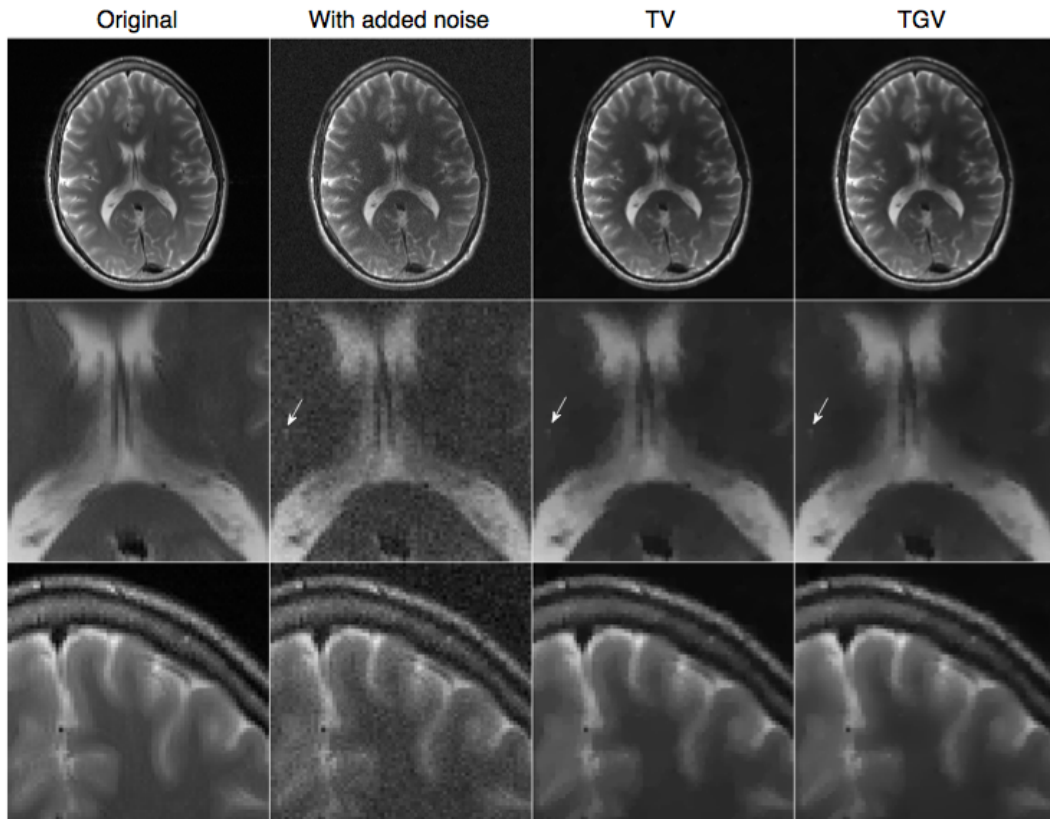
(c) ROF ($\lambda = 8$)



(d) $TV-L^1$ ($\lambda = 1.5$)

Source: Chambolle and Pock 2011.

Image Restoration



Classical TV vs second order total generalized variation (TGV) (Source: Knoll 2011).



1	2
3	4
5	6
7	8
9	10
11	12
13	14
15	16
17	18
19	20
21	22
23	24
25	26
27	28
29	30
31	32
33	34
35	36
37	38



Generalised Nonlocal Data and Smoothness Model

Pizarro *et al.* 2010

- ◆ Introduces a general metric $d(\cdot, \cdot)$ of dissimilarity:

$$E(u) = (1 - \alpha) \sum_{i,j \in J} \Psi_D \left(d^2(u_i, \textcolor{red}{f}_j) \right) w_D(|x_i - x_j|^2) \quad \text{Data similarity}$$

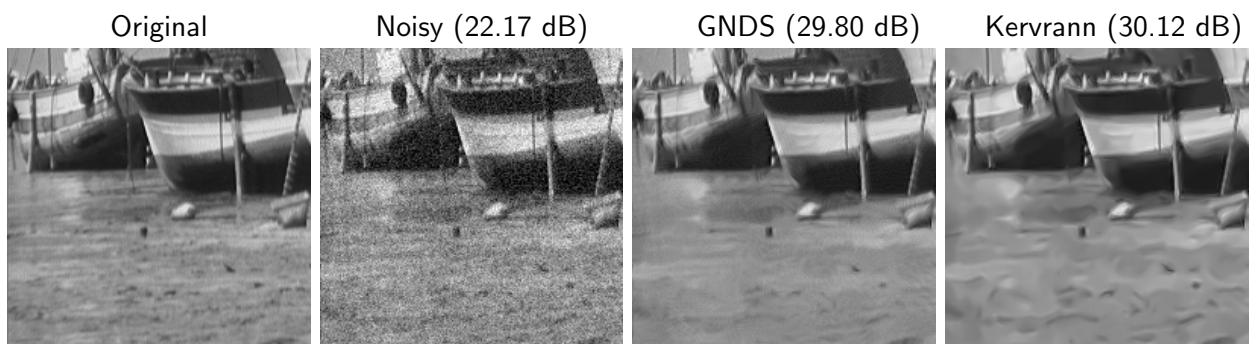
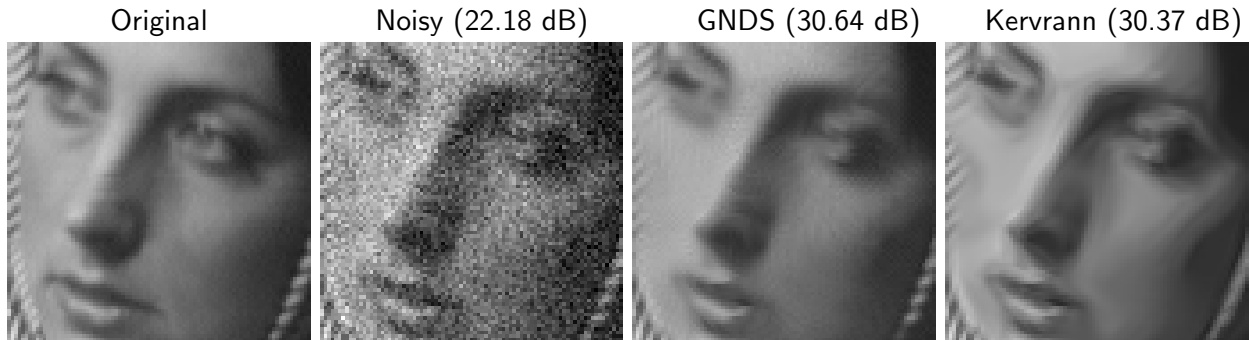
$$+ \alpha \sum_{i,j \in J} \Psi_S \left(d^2(u_i, \textcolor{blue}{u}_j) \right) w_S(|x_i - x_j|^2) \quad \text{Smoothness}$$

- ◆ Patch-based pixel dissimilarity can be measured by:

Distance	$d^2(u_i, u_j)$	Source
L_2	$\sum_q G_\sigma(q) u_{i+q} - u_{j+q} ^2$	Buades <i>et al.</i> (2005)
L_2^N	$\sum_q \sigma_{i,j}^{-1} u_{i+q} - u_{j+q} ^2$	Kervrann/Boulanger (2008)
Pearson	$\sum_q u_{j+q}^{-1} u_{i+q} - u_{j+q} ^2$	Coupé <i>et al.</i> (2008)



Examples



1	2
3	4
5	6
7	8
9	10
11	12
13	14
15	16
17	18
19	20
21	22
23	24
25	26
27	28
29	30
31	32
33	34
35	36
37	38

Image Restoration



Examples

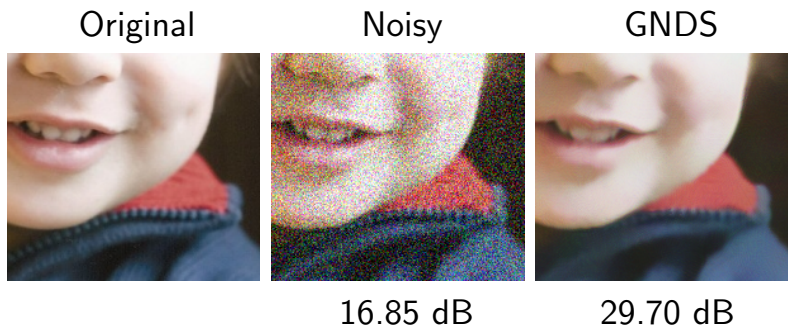


Image Restoration



Examples

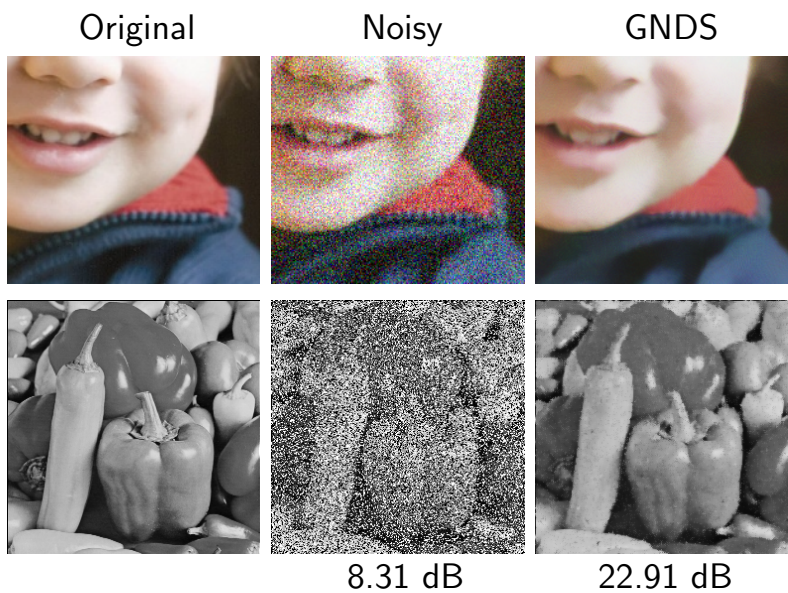
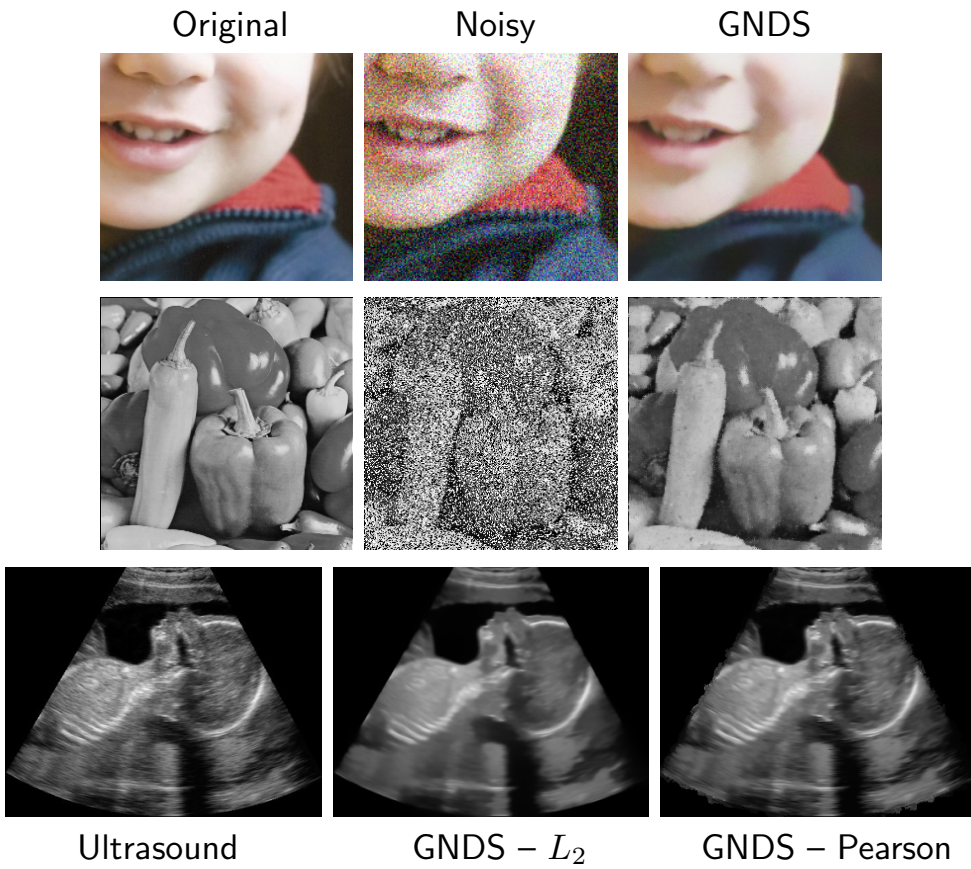


Image Restoration

Examples



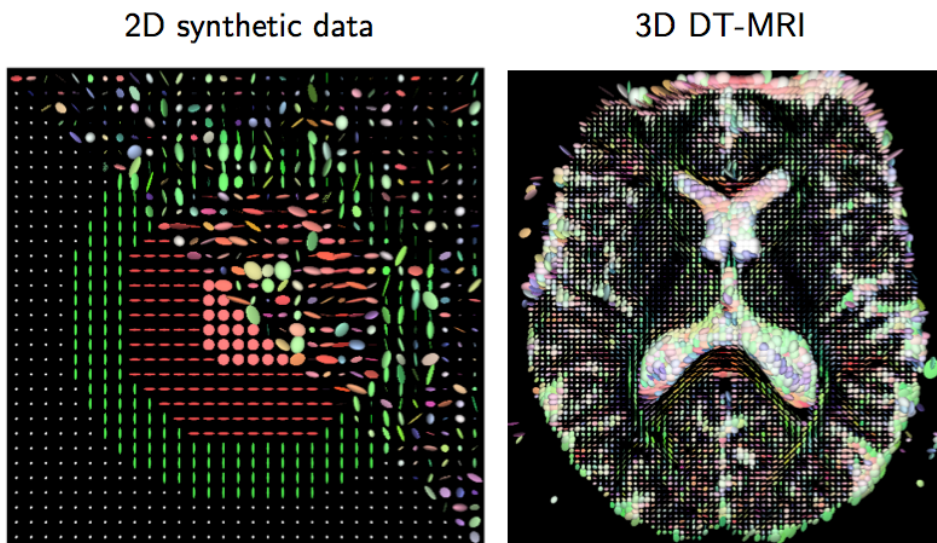
1	2
3	4
5	6
7	8
9	10
11	12
13	14
15	16
17	18
19	20
21	22
23	24
25	26
27	28
29	30
31	32
33	34
35	36
37	38

Image Restoration

Matrix-Valued NDS (MNDS)

(Pizarro/Burgeth/Didas/Weickert ECCV 2008, IEEE TIP submission 2011)

- ◆ Examples of matrix fields



1	2
3	4
5	6
7	8
9	10
11	12
13	14
15	16
17	18
19	20
21	22
23	24
25	26
27	28
29	30
31	32
33	34
35	36
37	38



◆ Isotropic MNDS Model:

$$E_i(U) = (1 - \alpha) \sum_{i,j \in J} \Psi_D \left(d^2(U_i, \mathbf{F}_j) \right) w_D(|x_i - x_j|^2) + \alpha \sum_{i,j \in J} \Psi_S \left(d^2(U_i, \mathbf{U}_j) \right) w_S(|x_i - x_j|^2)$$

◆ $d(A, B)$ measures dissimilarity between $A, B \in \text{Sym}_m(\mathbb{R})$:

Distance	$d(A, B)$
Euclidean	$d_E = \ A - B\ _F$
Log-Euclidean	$d_{LE} = \ \ln A - \ln B\ _F$
Affine-invariant	$d_{AI} = \left\ \ln \left(A^{-\frac{1}{2}} B A^{-\frac{1}{2}} \right) \right\ _F$

Image Restoration



Matrix-Valued NDS (MNDS)

(Pizarro/Burgeth/Didas/Weickert ECCV 2008, IEEE TIP submission 2011)

◆ Voxel dissimilarity measured as

Scalar NDS	Matrix NDS	type of method
$ u_i - \mathbf{f}_j \in \mathbb{R}^+$	$d(U_i, \mathbf{F}_j) \in \mathbb{R}^+$	isotropic
	$ U_i - \mathbf{F}_j \in \text{Sym}_m^+(\mathbb{R})$	anisotropic

Image Restoration



◆ Anisotropic MNDS Model:

$$E_a(U) = (1 - \alpha) \sum_{i,j \in J} \text{trace} \left(\Psi_D \left(|U_i - \mathbf{F}_j|^2 \right) \right) w_D (|x_i - x_j|^2) + \alpha \sum_{i,j \in J} \text{trace} \left(\Psi_S \left(|U_i - \mathbf{U}_j|^2 \right) \right) w_S (|x_i - x_j|^2)$$

◆ Related Filters for Matrix Fields:

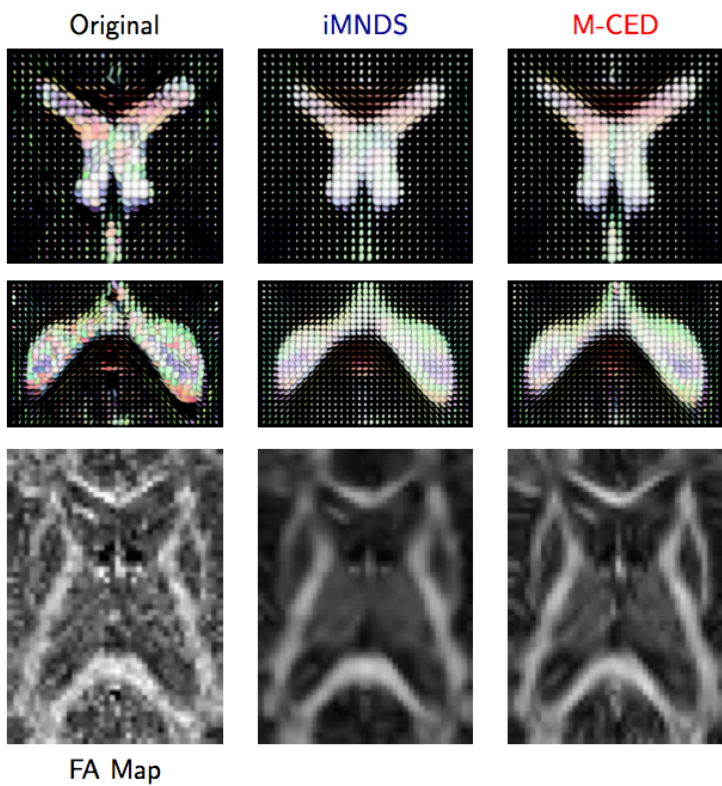
Filter	Source
M-smoothers, bilateral filtering	this thesis, Welk <i>et al.</i> (2007)
weighted average (d_{AI}, d_{LE})	Batchelor <i>et al.</i> (2005), Arsigny <i>et al.</i> (2006)
regularisation (d_{AI}, d_{LE})	Pennec <i>et al.</i> (2006), Fillard <i>et al.</i> (2007)
NL-means (d_{LE})	Wiest-Daesslé <i>et al.</i> (2007)
component-based regularisation (d_E)	Steidl <i>et al.</i> (2007), Setzer <i>et al.</i> (2009)
operator-based regularisation	Setzer <i>et al.</i> (2009)

1	2
3	4
5	6
7	8
9	10
11	12
13	14
15	16
17	18
19	20
21	22
23	24
25	26
27	28
29	30
31	32
33	34
35	36
37	38

Image Restoration



Denoising Example: 3D DT-MRI

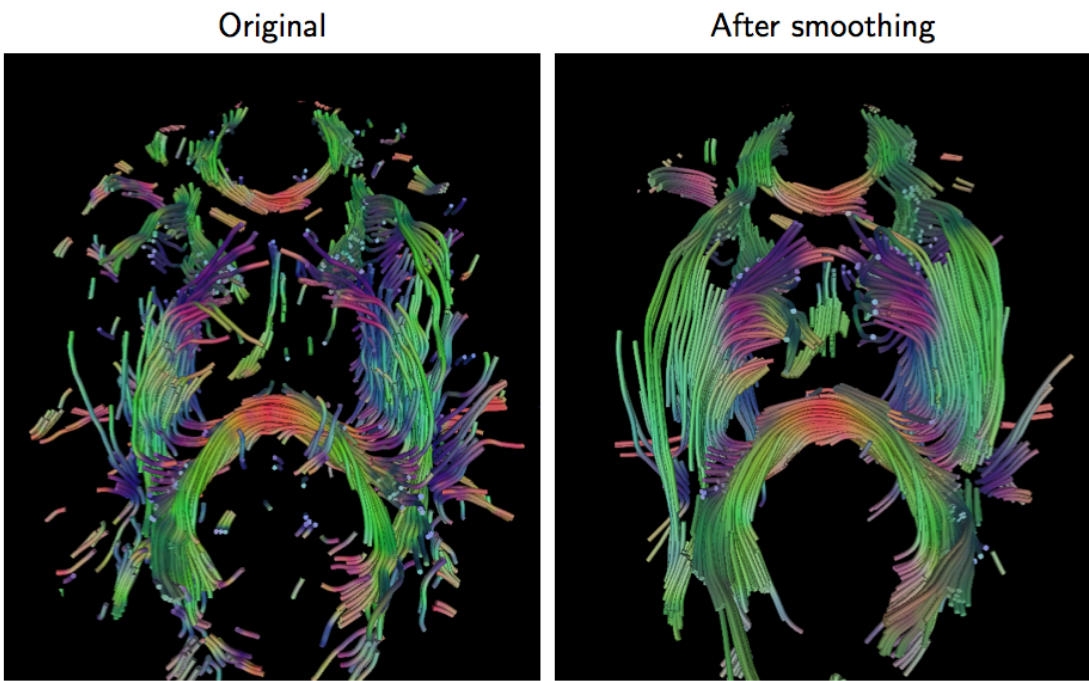


M-CED: Burgeth/Didas/Pizarro/Weickert (2009, 2011)

1	2
3	4
5	6
7	8
9	10
11	12
13	14
15	16
17	18
19	20
21	22
23	24
25	26
27	28
29	30
31	32
33	34
35	36
37	38



Tractography Example



Tractography algorithm courtesy of Thomas Schultz (University of Chicago)

Deblurring

Joint Interpolation, Deblurring and Smoothing

Persh *et al.* 2013

Denoising + Interpolation

$$E[u] := \int_{\Omega} (\chi_D \cdot (u - f)^2 + \alpha \cdot \Psi(|\nabla u|^2)) \, d\mathbf{x}$$

Here, the characteristic function

$$\chi_D : \Omega \rightarrow \{0, 1\}$$

is 1 where the information is known (inside D) and 0 everywhere else.

Assumption: photon impacts follow a Poisson distribution. Then, the probability $p(f|g)$ of acquiring the image f , given that the true object is g , reads

$$p(f|g) = \prod_{\mathbf{x} \in D} \left(\frac{((h * g)(\mathbf{x}))^{f(\mathbf{x})}}{f(\mathbf{x})!} e^{-(h * g)(\mathbf{x})} \right)$$



1	2
3	4
5	6
7	8
9	10
11	12
13	14
15	16
17	18
19	20
21	22
23	24
25	26
27	28
29	30
31	32
33	34
35	36
37	38

Deblurring

Joint Interpolation, Deblurring and Smoothing

Persh *et al.* 2013

It follows the variational model

$$E_{f,h}^{\text{RL}}[u] := \int_D \left((h * u - f) - f \cdot \ln \left(\frac{h * u}{f} \right) \right) dx$$

Its regularised version

$$E_{f,h}^{\text{RRL}}[u] := \int_D \left(\underbrace{h * u - f - f \ln \left(\frac{h * u}{f} \right)}_{\text{deconvolution}} + \underbrace{\alpha \cdot \Psi(|\nabla u|^2)}_{\text{smoothness}} \right) dx$$

Its robust version

$$E_{f,h}^{\text{RRRL}}[u] := \int_D \left(\underbrace{\Phi \left(h * u - f - f \ln \left(\frac{h * u}{f} \right) \right)}_{=: r_f(h*u)} + \alpha \cdot \Psi(|\nabla u|^2) \right) dx$$

leads to the PDE

$$\left(h^* * \left(\chi_D \cdot \Phi'(r_f(u * h)) \left(1 - \frac{f}{u * h} \right) \right) - \alpha \cdot \operatorname{div}(\Psi'(|\nabla u|^2) \nabla u) \right) \cdot u = 0$$



1 2

3 4

5 6

7 8

9 10

11 12

13 14

15 16

17 18

19 20

21 22

23 24

25 26

27 28

29 30

31 32

33 34

35 36

37 38

Deblurring

Joint Interpolation, Deblurring and Smoothing

Persh *et al.* 2013

It follows the variational model

$$E_{f,h}^{\text{RL}}[u] := \int_D \left((h * u - f) - f \cdot \ln \left(\frac{h * u}{f} \right) \right) dx$$

Its regularised version

$$E_{f,h}^{\text{RRL}}[u] := \int_D \left(\underbrace{h * u - f - f \ln \left(\frac{h * u}{f} \right)}_{\text{deconvolution}} + \underbrace{\alpha \cdot \Psi(|\nabla u|^2)}_{\text{smoothness}} \right) dx$$

Its robust version

$$E_{f,h}^{\text{RRRL}}[u] := \int_D \left(\underbrace{\Phi \left(h * u - f - f \ln \left(\frac{h * u}{f} \right) \right)}_{=: r_f(h*u)} + \alpha \cdot \Psi(|\nabla u|^2) \right) dx$$



1 2

3 4

5 6

7 8

9 10

11 12

13 14

15 16

17 18

19 20

21 22

23 24

25 26

27 28

29 30

31 32

33 34

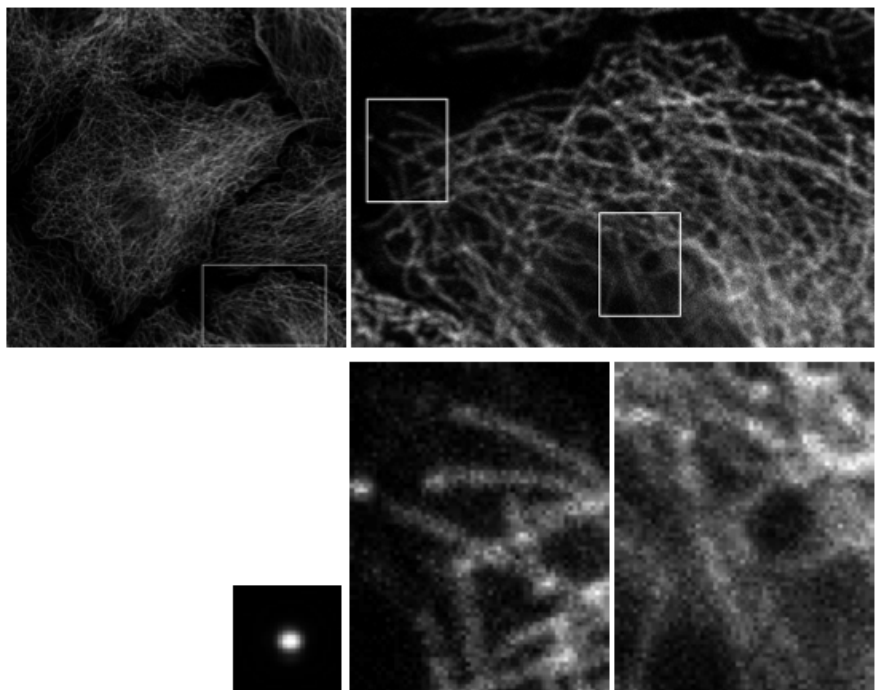
35 36

37 38

leads to the PDE

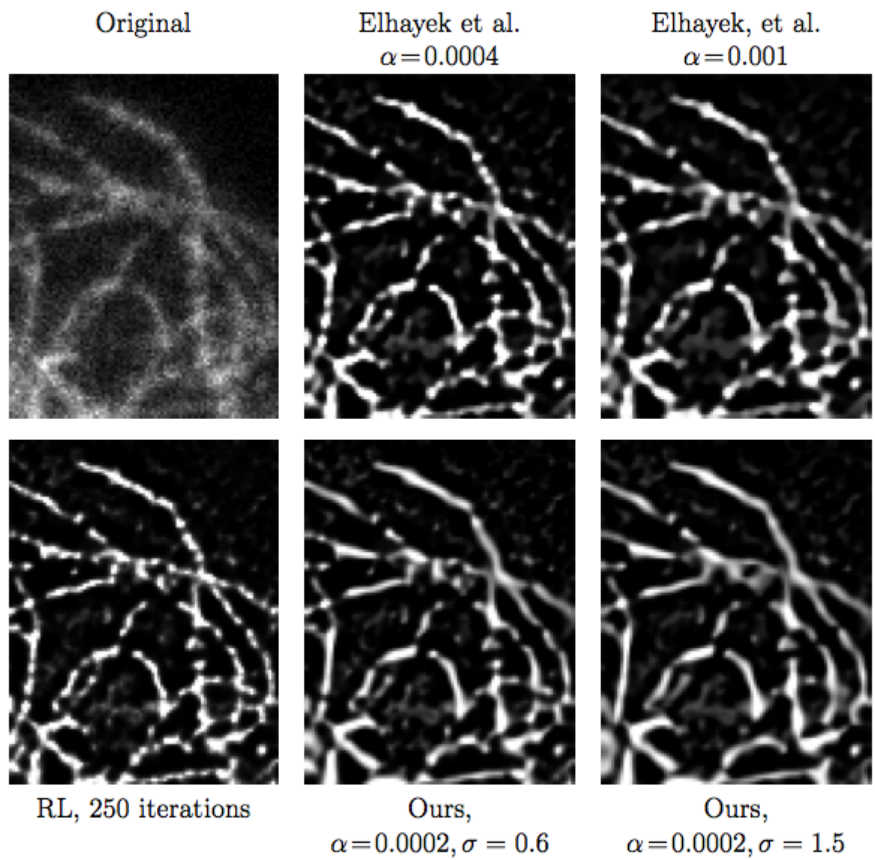
$$\left(h^* * \left(\chi_D \cdot \Phi'(r_f(u * h)) \left(1 - \frac{f}{u * h} \right) \right) - \alpha \cdot \operatorname{div}(\Psi'(|\nabla u|^2) \nabla u) \right) \cdot u = 0$$

Optic Flow



1	2
3	4
5	6
7	8
9	10
11	12
13	14
15	16
17	18
19	20
21	22
23	24
25	26
27	28
29	30
31	32
33	34
35	36
37	38

Optic Flow



1	2
3	4
5	6
7	8
9	10
11	12
13	14
15	16
17	18
19	20
21	22
23	24
25	26
27	28
29	30
31	32
33	34
35	36
37	38

Optic Flow



Basic Model

Horn and Schunk 1981

Compute the motion field $(u, v)^\top$ between two images I_1 and I_2 assuming brightness constancy and isotropic flow regularisation

$$0 = \frac{dI(u(t), v(t), t)}{dt} \\ = I_x u + I_y v + I_t \quad \text{with } I_t = I_2 - I_1$$

$$\min_{u,v} \int_{\Omega} \left((I_x u + I_y v + I_t)^2 + \alpha \Psi(|\nabla u|^2 + |\nabla v|^2) \right) dx$$

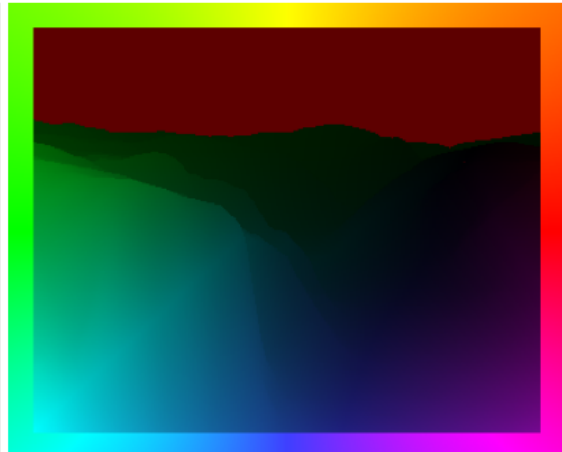
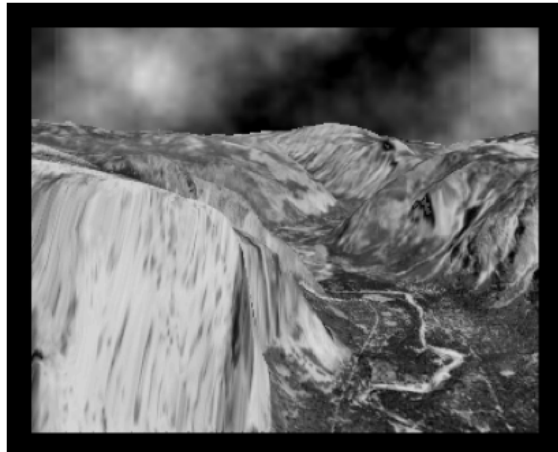
Possible penalisers: $\Psi(s^2) = s^2$, $\Psi(s^2) = |s|$

Solution via the coupled PDEs

$$\frac{\partial u}{\partial t} = \operatorname{div} (\Psi'(|\nabla u|^2 + |\nabla v|^2) \nabla u) - \frac{1}{\alpha} I_x (I_x u + I_y v + I_t) \\ \frac{\partial v}{\partial t} = \operatorname{div} (\Psi'(|\nabla u|^2 + |\nabla v|^2) \nabla v) - \frac{1}{\alpha} I_y (I_x u + I_y v + I_t)$$

1	2
3	4
5	6
7	8
9	10
11	12
13	14
15	16
17	18
19	20
21	22
23	24
25	26
27	28
29	30
31	32
33	34
35	36
37	38

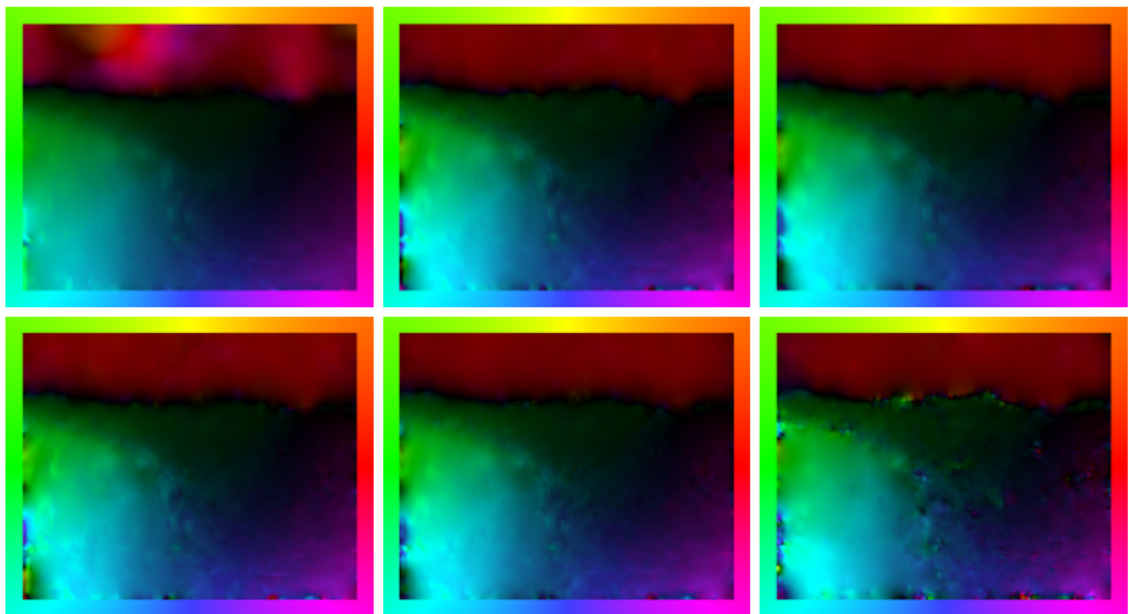
Optic Flow



(a) **Left:** Frame 8 of the *Yosemite sequence with clouds*, depicting translatory and divergent motion, 316 × 256 pixels. (b) **Right:** Ground truth flow field, colour-coded.

1	2
3	4
5	6
7	8
9	10
11	12
13	14
15	16
17	18
19	20
21	22
23	24
25	26
27	28
29	30
31	32
33	34
35	36
37	38

Optic Flow



(a) **Top left:** Colour-coded flow field with the data term M_1 (brightness constancy) and a spatial Horn-Schunck regulariser. (b) **Top middle:** Data term M_2 (gradient constancy). (c) **Top right:** Data term M_3 (Hessian constancy). (d) **Bottom left:** Data term M_4 (constancy of gradient magnitude). (e) **Bottom middle:** Data term M_5 (constancy of Laplacian). (f) **Bottom right:** Data term M_6 (constancy of Hessian determinant). Author: A. Bruhn (2006)

Optic Flow

TV-L1 Model

Chambolle and Pock 2011

$$\min_{u,v} \left(\|\nabla u\| + \|\nabla v\| + \lambda \|\rho(u,v)\| \right)$$

with $\rho(u,v) = I_x u + I_y v + I_t$

- ◆ Discrete primal-dual

$$\min_u \max_p \left\{ \langle Du, p \rangle + G(u) - F^*(p) \right\}$$

reads

$$\min_{u \in X, v \in Y} \max_{p \in Y, q \in Z} \left(\langle \nabla u, p \rangle_Y + \langle \nabla v, q \rangle_Z + \lambda \|\rho(u,v)\| - \delta_P(p) - \delta_Q(q) \right)$$



1	2
3	4
5	6
7	8
9	10
11	12
13	14
15	16
17	18
19	20
21	22
23	24
25	26
27	28
29	30
31	32
33	34
35	36
37	38

Optic Flow

Then

$$\min_{u \in X, v \in Y} \max_{p \in Y, q \in Z} \left(< \nabla u, p >_Y + < \nabla v, q >_Z + \lambda \| \rho(u, v) \| - \delta_P(p) - \delta_Q(q) \right)$$

$$(p, q) = (I + \sigma \partial F^*)^{-1}(\tilde{p}, \tilde{q}) \iff p_{i,j} = \frac{\tilde{p}_{i,j}}{\max(1, |\tilde{p}_{i,j}|)}, q_{i,j} = \frac{\tilde{q}_{i,j}}{\max(1, |\tilde{q}_{i,j}|)}$$

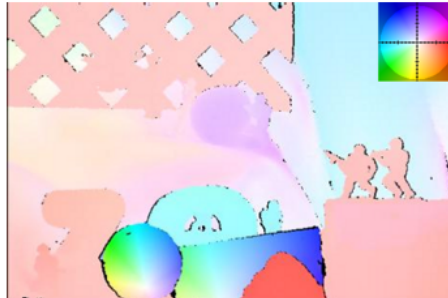
$$(u, v) = (I + \tau \partial G)^{-1}(\tilde{u}, \tilde{v}) \iff (u_{i,j}, v_{i,j}) = (\tilde{u}_{i,j}, \tilde{v}_{i,j})$$

$$+ \begin{cases} \tau \lambda a_{i,j} & \text{if } \rho(\tilde{u}_{i,j}, \tilde{v}_{i,j}) < -\tau \lambda |a|_{i,j}^2 \\ -\tau \lambda a_{i,j} & \text{if } \rho(\tilde{u}_{i,j}, \tilde{v}_{i,j}) > \tau \lambda |a|_{i,j}^2 \\ -\rho(\tilde{u}_{i,j}, \tilde{v}_{i,j}) a_{i,j} / |a|_{i,j}^2 & \text{if } |\rho(\tilde{u}_{i,j}, \tilde{v}_{i,j})| \leq \tau \lambda |a|_{i,j}^2 \end{cases}$$

Optic Flow



(a) First frame



(b) Ground truth



(c) Illumination



(d) Motion



1	2
3	4
5	6
7	8
9	10
11	12
13	14
15	16
17	18
19	20
21	22
23	24
25	26
27	28
29	30
31	32
33	34
35	36
37	38



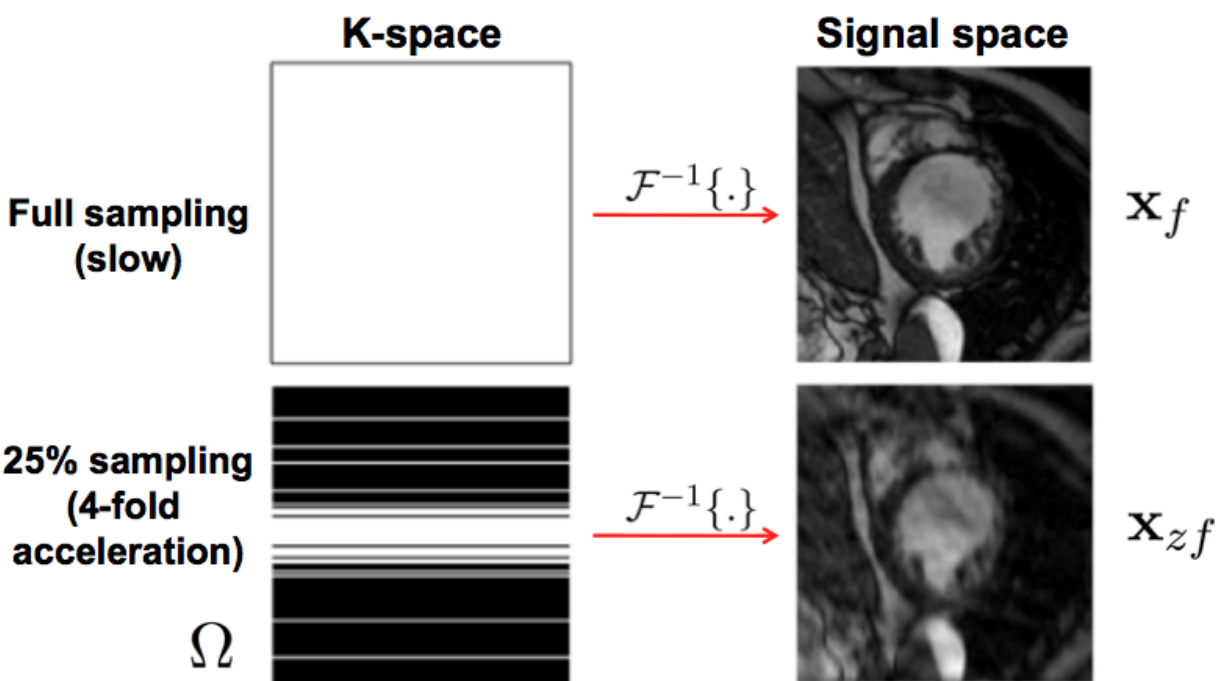
1	2
3	4
5	6
7	8
9	10
11	12
13	14
15	16
17	18
19	20
21	22
23	24
25	26
27	28
29	30
31	32
33	34
35	36
37	38

Reconstruction

Cardiac MRI reconstruction



1	2
3	4
5	6
7	8
9	10
11	12
13	14
15	16
17	18
19	20
21	22
23	24
25	26
27	28
29	30
31	32
33	34
35	36
37	38



Reconstruction

Cardiac MRI reconstruction

Caballero *et al.* 2012



1	2
3	4
5	6
7	8
9	10
11	12
13	14
15	16
17	18
19	20
21	22
23	24
25	26
27	28
29	30
31	32
33	34
35	36
37	38

Step 1: Local patch sparse coding

$$\min_{\Gamma} \|\gamma_j\|_0 \quad s.t. \quad \|\mathbf{R}_j \mathbf{y} - \mathbf{D} \gamma_j\|_2^2 < \epsilon, \forall j$$

$$\mathbf{y} = \frac{\sum_{j=1}^P \mathbf{R}_j^T \mathbf{D} \gamma_j}{n}$$

Step 2: Global TG sparse coding

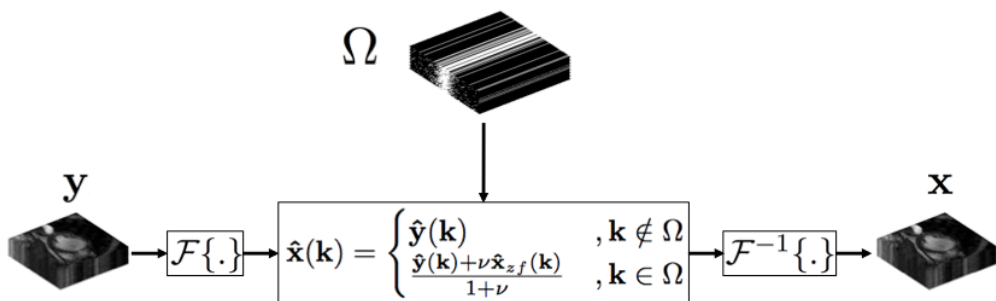
$$\min_{\mathbf{x}} \lambda \|\nabla_t \{\mathbf{x}\}\|_1 + \frac{1}{2} \|\mathbf{y} - \mathbf{x}\|_2^2$$

Reconstruction

Cardiac MRI reconstruction

Caballero *et al.* 2012

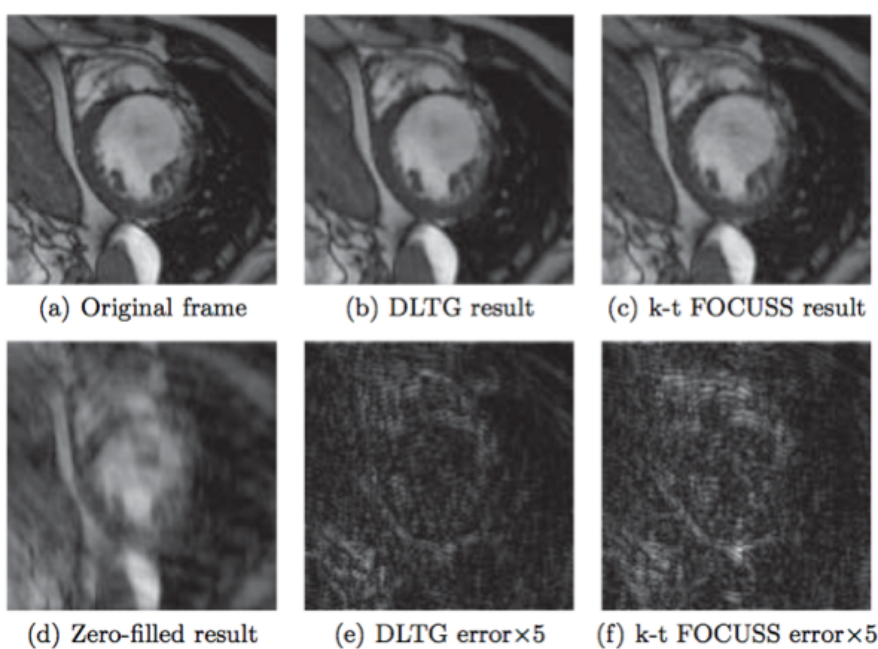
Step 3: Data consistency in k-space



Reconstruction

Cardiac MRI Reconstruction

Caballero *et al.* 2012



1	2
3	4
5	6
7	8
9	10
11	12
13	14
15	16
17	18
19	20
21	22
23	24
25	26
27	28
29	30
31	32
33	34
35	36
37	38



Motion-Adaptive Reconstruction

Asif *et al.* 2012

MASTeR

- Inter-frame motion estimation/compensation

$$\left. \begin{array}{l} \mathbf{y}_i = \mathcal{A}_i \mathbf{x}_i + \mathbf{e}_i \\ \mathbf{x}_i = \mathbf{F}_{i-1} \mathbf{x}_{i-1} + \mathbf{f}_i \\ \mathbf{x}_i = \mathbf{B}_{i+1} \mathbf{x}_{i+1} + \mathbf{b}_i \end{array} \right\} \quad \begin{array}{l} \mathbf{f}_i = \mathbf{F}_{i-1} \mathbf{x}_{i-1} - \mathbf{x}_i \\ \mathbf{b}_i = \mathbf{B}_{i+1} \mathbf{x}_{i+1} - \mathbf{x}_i \end{array}$$

\mathbf{F}_{i-1} , \mathbf{B}_{i+1} : FW and BW motion operator

\mathbf{f}_i , \mathbf{b}_i : FW and BW motion-compensated residuals



Motion-Adaptive Reconstruction

Asif *et al.* 2012

MASTeR – iteratively solves:

- Initialisation

$$\underset{\mathbf{x}}{\text{minimize}} \sum_i \|\mathcal{A}_i \mathbf{x}_i - \mathbf{y}_i\|_2^2 + \tau \|\Psi \mathbf{x}_i\|_1$$

↑
wavelet transform

- Motion adaptation

– Motion estimation: Use reconstructed \mathbf{x}_i to estimate \mathbf{F}_i , \mathbf{B}_i with, e.g., an optical-flow method

– Motion compensation:

$$\underset{\mathbf{x}}{\text{minimize}} \sum_i \|\mathcal{A}_i \mathbf{x}_i - \mathbf{y}_i\|_2^2 + \alpha \|\mathbf{F}_{i-1} \mathbf{x}_{i-1} - \mathbf{x}_i\|_1 + \beta \|\mathbf{B}_{i+1} \mathbf{x}_{i+1} - \mathbf{x}_i\|_1$$

1	2
3	4
5	6
7	8
9	10
11	12
13	14
15	16
17	18
19	20
21	22
23	24
25	26
27	28
29	30
31	32
33	34
35	36
37	38



Motion-Adaptive Reconstruction

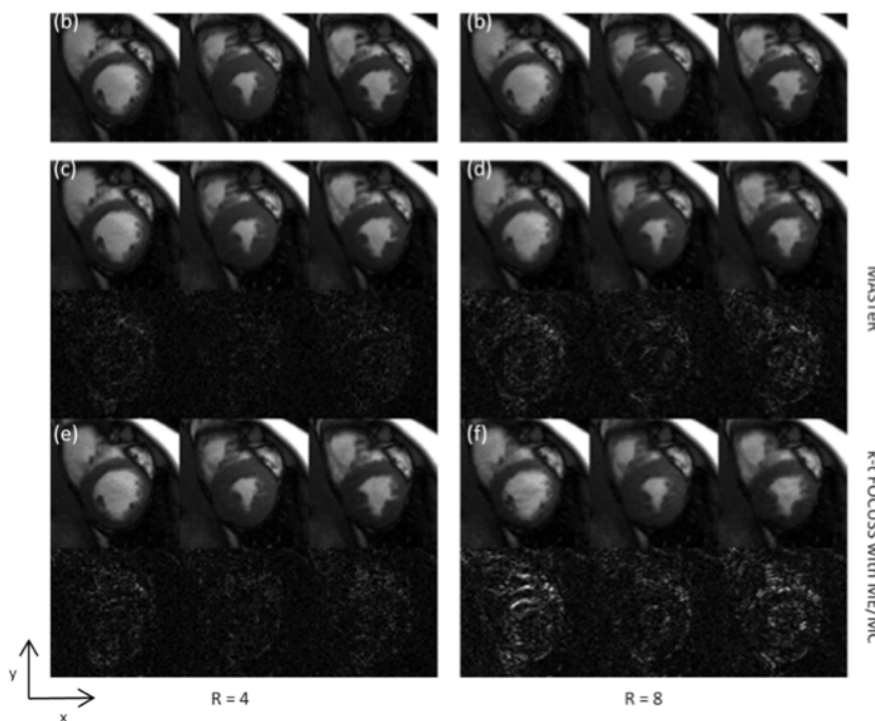
Asif *et al.* 2012

Results

True images

MASTeR

$k\text{-}t$ FOCUSS with ME/MC



References

- ◆ S. Didas: Higher order variational methods for noise removal in signals and images. Diploma Thesis, Department of Mathematics, Saarland University, 2004.
- ◆ L. Rudin, S. J. Osher, E. Fatemi: Nonlinear total variation based noise removal algorithms. *Physica D*, 60:259–268, 1992.
- ◆ A. Chambolle, T. Pock: A first-order primal-dual algorithm for convex problems with applications to imaging. *Journal of Mathematical Imaging and Vision*, Vol. 40, No. 1, 120–145, 2011.
- ◆ F. Knoll, K. Bredies, T. Pock, R. Stollberger: Second order total generalized variation (TGV) for MRI. *Magnetic Resonance in Medicine*, Vol. 65, No. 2, 480–491, 2011.
- ◆ L. Pizarro, P. Mrázek, S. Didas, S. Grewenig, J. Weickert: Generalised nonlocal image smoothing. *International Journal of Computer Vision*, Vol. 90, No. 1, 62–87, 2010.
- ◆ L. Pizarro, B. Burgeth, S. Didas, J. Weickert: A generic neighbourhood filtering framework for matrix fields. *European Conference on Computer Vision (ECCV)*, Lecture Notes in Computer Science, Vol. 5304, 521–532. Springer, Berlin, 2008.
- ◆ N. Persch, A. Elhayek, M. Welk, A. Bruhn, S. Grewenig, K. Böse, A. Kraegeloh, J. Weickert: Enhancing 3-D cell structures in confocal and STED microscopy: A joint model for interpolation, deblurring and anisotropic smoothing. *Measurement Science and Technology*, in press, 2013.
- ◆ B. Horn, B. Schunck: Determining optical flow. *Artificial Intelligence*, Vol. 17, 185–203, 1981.
- ◆ J. Caballero, D. Rueckert, J. V. Hajnal: Dictionary learning and time sparsity for dynamic MRI. *International Conference on Medical Imaging Computing and Computer Assisted Interventions (MICCAI)*, Vol. 1, 256–263, 2012.
- ◆ M. S. Asif, L. Hamilton, M. Brummer, J. Romberg: Motion-Adaptive Spatio-Temporal Regularization for Accelerated Dynamic MRI. *Magnetic Resonance in Medicine*, Vol. 70, No. 3, 800–812, 2013.

1	2
3	4
5	6
7	8
9	10
11	12
13	14
15	16
17	18
19	20
21	22
23	24
25	26
27	28
29	30
31	32
33	34
35	36
37	38



1	2
3	4
5	6
7	8
9	10
11	12
13	14
15	16
17	18
19	20
21	22
23	24
25	26
27	28
29	30
31	32
33	34
35	36
37	38